15th ASCE Engineering Mechanics Conference
June 2-5, 2002, Columbia University, New York, NY

MULTI-SCALE UNIT CELL ANALYSES OF TEXTILE COMPOSITES

Colby C. Swan[1], Member ASCE
and HyungJoo Kim[2]

ABSTRACT

Unit cell homogenization techniques are applied on multiple length scales to compute the macroscopic hyperelastic stiffness characteristics of textile-reinforced polymer matrix composites. On the smallest scale (~50μm) the effective transversely isotropic properties of tows (or yarns) are computed based on both fiber and matrix properties. These position-dependent transversely isotropic effective yarn properties are then incorporated into a full textile unit cell model and the nonlinear effective stiffness properties of the textile composite are computed and discussed.

Keywords: FRPs; homogenization; woven-fabric composites; textile composites; finite deformation; unit cell analysis.

INTRODUCTION

Unit cell computational homogenization methods typically involve constructing a continuum model of a composite's heterogeneous material structure and then applying loads to the model with imposed periodic boundary conditions (e.g. Swan, 1994, 1997). When applied to composites undergoing finite deformations, unit cell analysis can be performed by assuming periodicity of both stress and deformation fields on the appropriate material scale or microscale. This assumption of periodicity is indeed likely to be valid up until the point where deformation becomes highly localized due to fiber or yarn buckling. Textile reinforced composites, also referred to as woven fabric composites are hierarchical (Fig. 1) in that they feature heterogeneity and structure on a variety of length scales, specifically a) the fiber diameter scale; b) the yarn-diameter scale; c) the textile unit cell scale; and d) the structural element scale. When attempting to analyze structures that utilize textile or woven fabric composites (WFCs), a number of different modeling approaches have been taken to account for the material hierarchy. For the sake of brief review, these approaches can be classified into those that develop analytical macro-scale constitutive models for the nonlinear, hierarchical composites, and those that do not.

Among the works that do not utilize analytical effective medium constitutive models is that of Tabiei et al (1999, 2000) who performed analysis of shell structures fabricated with WFCs, but used a structural subcell technique based on local textile material structure and weighted rules of mixtures to compute stress response to structural scale strains in the shell model. Concurrent global structural shell analysis and local analysis have also been performed by Peng and Cao

[1] Dept. of Civil & Env. Engng. CCAD, University of Iowa, Iowa City, IA 52242. Colby-swan@uiowa.edu.
[2] Dept. of Mech & Indust. Engng., CCAD, University of Iowa, Iowa City, IA 52242. Hkim@engineering.uiowa.edu.

(2001) who for their local analysis used tabulated results from unit cell analysis of plain-weave composites. Similar concurrent multi-scale analysis techniques have also been investigated by Fish and Shek (2000) and Takano et al (2001) who have attempted to address the geometrical nonlinear effects that occur in textile composites. An important issue with concurrent multi-scale analysis is minimizing the computational cost of calculating micro-structural stress and strain fields during global structural analysis.

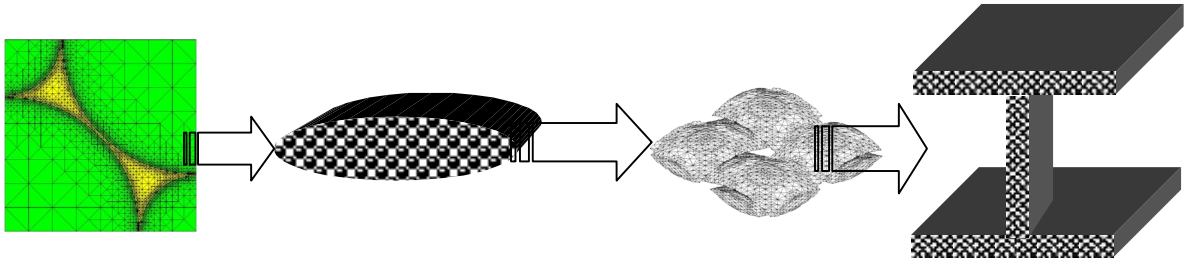

a) b) c) d)

Figure 1. Multiple scales in textile composites, including: a) fiber-diameter scale; b) yarn-diameter scale; c) textile-unit cell scale; and d) structural scale.

When the length scale associated with variations of macro-scale structural deformation are much larger than the unit cell dimensions associated with material structure on a finer scale, the effective medium approximation will be valid. In this case, one can effectively model the composite using a constitutive model that relates the homogenized strain and stress measures that derive from spatial averaging of their microscale counterparts. In this work, unit cell analysis of an aligned-fiber composite is performed and then used to calibrate a transversely isotropic hyperelasticity model. This transversely isotropic hyperelasticity model is then employed in unit cell models for a plain-weave textile to compute nonlinear stress-strain behaviors associated with finite deformation hyperelastic behaviors.

Much of the preceding research on modeling of transversely-isotropic hyperelastic materials has been devoted to developing appropriate mathematical forms and to estimation of free parameters to fit experimentally measured material responses such as those of fibrous biological tissues (Weiss et al, 1996). The experimental behavior of fibrous biological tissues wherein the fibers are initially in a wavy, undulating arrangement, features increasing elastic stiffness under uniaxial tensile loading, and decreasing stiffness under uniaxial compressive loading. Here, the transversely-isotropic neo-Hookean constitutive model of Bonet and Burton (1998) is employed to reproduce such homogenized stress-strain behavior of aligned-fibers within the warped yarns of a plain-weave textile composite. The macro-scale nonlinear stress-strain behaviors of the textile composite are then computed with unit cell analysis at finite deformations.

SYMMETRIC, CONJUGATE MEASURES FOR AVERAGED STRAIN AND STRESS

When dealing with homogenized stain or stress measures of composites undergoing finite deformations, it is important that they be conjugate to each other. For example, Nemat-Nasser (2000) has shown that the volume averages of the rate of deformation gradient $d\boldsymbol{F}/dt$ and nominal stress $\boldsymbol{P}$ satisfy the following conjugacy identity which assures conservation of energy in the homogenization process:

$$\left\langle P_{Ji}\dot{F}_{iJ}\right\rangle = \left\langle P_{Ji}\right\rangle\left\langle \dot{F}_{iJ}\right\rangle \tag{1}$$

Since both the nominal stress **P** and the rate of deformation gradient d***F***/dt are non-symmetric, it is preferred here to develop constitutive models using symmetric conjugate measures. Accordingly, it can be demonstrated (Kim, 2002) that the following conjugacy relations hold:

$$\hat{S}_{IJ}\dot{\hat{E}}_{IJ} = \left\langle P_{Ji}\right\rangle\left\langle \dot{F}_{iJ}\right\rangle = \left\langle P_{Ji}\dot{F}_{iJ}\right\rangle = \left\langle S_{IJ}\dot{E}_{IJ}\right\rangle \tag{2}$$

In the preceding, S_{IJ} denotes the second Piola Kirchoff stress tensor on the material scale, and E_{IJ} denotes the Green-Lagrange strain tensor on the material scale. Similarly, the following averaged quantities in (2) are here defined as follows:

$$\hat{S}_{IJ} = \left\langle S_{IJ}\right\rangle; \qquad \hat{E}_{IJ} = \tfrac{1}{2}(\hat{F}_{iI}\hat{F}_{iJ} - \delta_{IJ}); \qquad \hat{F}_{iJ} = \left\langle F_{iJ}\right\rangle \tag{3}$$

UNIT CELL HOMOGENIZATION

The composite materials under consideration here are assumed to occupy a domain Ω_b in $\Re^3$ and to exhibit periodic microstructures in that a single wavelength sub-domain forms a unit cell $\Omega_s = \Pi_{i=1}^{3}]0,\lambda_i[$, where λ_i are the dimensions of a specific composite's unit cell. Regions of the structural domain Ω_b are formed by repetition of a specific composite's unit cell Ω_s. Material points in an undeformed unit cell Ω_s are referenced by local material scale coordinates **X**, while the spatial material scale coordinates **x** locate material points in a deformed cell. Similarly, the Lagrangian and spatial macro-scale coordinates of a point in the larger domain Ω_b are denoted by **Y** and **y**. The undeformed and deformed locations of a material point are related by displacement vectors **u** such that

$$\mathbf{x} = \mathbf{X} + \mathbf{u(X)} \text{ material scale;} \qquad \mathbf{y} = \mathbf{Y} + \mathbf{u(Y)} \text{ macro scale.} \tag{4}$$

Material scale coordinates ***X*** and x are used in solving unit cell homogenization problems on one scale, whereas macroscale coordinates ***Y*** and ***y*** are used in solving structural analysis problems with the effective medium approximation on a larger scale.

At the material scale, and at the macroscale, the respective deformation gradients are defined as follows:

$$\mathbf{F}(\mathbf{X},\mathbf{Y}) = \frac{\partial \mathbf{x}}{\partial \mathbf{X}}; \qquad \hat{\mathbf{F}}(\mathbf{Y}) = \frac{\partial \mathbf{y}}{\partial \mathbf{Y}} = \left\langle \mathbf{F}(\mathbf{X},\mathbf{Y})\right\rangle \tag{5}$$

If the length scale of variation ℓ associated with macroscopic deformation **<F>** in a composite domain Ω_b is much larger than the wavelengths λ of the material microstructure ($l/|\lambda|>>1$) then the deformation and stress fields will be λ-periodic on the material scale. The periodicity of the stress and deformation fields on the material–scale suggests that they admit additive decompositions into macroscopic contributions $(\hat{\mathbf{S}},\hat{\mathbf{F}})$ defined in (3), which are constant on the micro-scale and vary slowly on the macroscale, and purely oscillatory contributions [**S*(X), F*(X)**], which can vary quite significantly on the unit cell length scale:

$$\mathbf{S}(\mathbf{X},\mathbf{Y}) = \hat{\mathbf{S}}(\mathbf{Y}) + \mathbf{S}^*(\mathbf{X},\mathbf{Y}); \qquad \mathbf{F}(\mathbf{X},\mathbf{Y}) = \hat{\mathbf{F}}(\mathbf{Y}) + \mathbf{F}^*(\mathbf{X},\mathbf{Y}). \tag{6}$$

With regard to the constant-periodic decomposition of the deformation field on the microscale (6b), it can also be shown by integrating (5a) that the displacement field on the microscale associated with a state of macroscopic deformation $\hat{\mathbf{F}}$ satisfies the linear-periodic decomposition

$$\mathbf{u}(\mathbf{X}) = \left[\hat{\mathbf{F}} - \mathbf{1}\right] \cdot \mathbf{X} + \mathbf{u}^*_{\text{per}}(\mathbf{X}) \tag{7}$$

where any constant or rigid body contributions to the displacement field **u** are eliminated by proper restraints on the unit cell domain, and imposing $\hat{\mathbf{F}} = \mathbf{R} \cdot \mathbf{U}$, where **R** is a rotation operator, and **U** is the right stretch tensor. The periodic displacement field contribution $\mathbf{u}^*_{\text{per}}(\mathbf{X})$ permits a heterogeneous (non-uniform) deformation field within the unit cell domain $\overline{\Omega}_s$, satisfying local stress equilibrium.

The deformation-controlled homogenization problem involves imposing macroscopic deformation <**F**> (or imposing $\mathbf{u} = [<\mathbf{F}> - \mathbf{1}] \cdot \mathbf{X}$) on the cell of a composite and computing the resulting periodic minimal energy displacement field $\mathbf{u}^*: \Omega_s \Rightarrow \Re^3$ satisfying the equilibrium equation. From the equilibrium local displacement field **u(X)**, strain-displacement relations, and constitutive behaviors of the materials in the composites, the corresponding stress field **S**(**X**) and its macroscopic counterpart $\hat{\mathbf{S}}$ can be computed.

While there are numerous transversely isotropic hyperelasticity models presented in the literature, we here use that presented by Bonet and Burton (1998) as a point of departure. In this model, a hyper-elastic potential ψ for transversely-isotropic materials is assumed to have an additive decomposition into an isotropic potential and a transversely isotropic potential:

$$\psi = \psi(\mathrm{I}_1, \mathrm{I}_2, \mathrm{I}_3, \mathrm{I}_4, \mathrm{I}_5) = \psi_{\text{inh}} + \psi_{\text{ti}} \tag{8}$$

where

$$\mathrm{I}_1 = \mathrm{tr}(\mathbf{C}); \quad \mathrm{I}_2 = \mathbf{C} : \mathbf{C}; \quad \mathrm{I}_3 = \det(\mathbf{C}) = \mathrm{J}^2; \quad \mathrm{I}_4 = \mathbf{A} \cdot \mathbf{C} \cdot \mathbf{A}; \quad \mathrm{I}_5 = (\mathbf{A} \cdot \mathbf{C}) \cdot (\mathbf{C} \cdot \mathbf{A}) \tag{9}$$

A is a unit normal vector to the transverse plane of symmetry in the undeformed state, and **C** is the right Cauchy-Green deformation tensor. The isotropic and transversely isotropic portions of the strain energy functions take the following specific forms:

$$\psi_{\text{inh}} = \tfrac{1}{2}\mu(\mathrm{I}_1 - 3) - \mu \ln \mathrm{J} + \tfrac{1}{2}\lambda(\mathrm{J} - 1)^2 \tag{10}$$

$$\psi_{\text{ti}} = [\alpha + \beta \ln \mathrm{J} + \gamma(\mathrm{I}_4 - 1)](\mathrm{I}_4 - 1) - \tfrac{1}{2}\alpha(\mathrm{I}_5 - 1) \tag{11}$$

where λ, μ, α, β, γ are the free parameters.

The results of unit cell analysis computations can be used to estimate the five coefficients in the proposed hyperelastic material model. Specifically, under deformation controlled loading, the material parameters $\boldsymbol{\alpha}$ can be selected to minimize stress-space error between the homogenized stresses $\hat{\mathbf{S}}$ and the stresses produced by the proposed material model and a set of material parameters $\tilde{\mathbf{S}}(\boldsymbol{\alpha})$:

$$\min_{\boldsymbol{\alpha}} \sum_k \int_{t_1}^{t_2} \left\| \frac{\hat{\mathbf{S}}^k(\tau) - \tilde{\mathbf{S}}^k(\boldsymbol{\alpha}, \tau)}{\hat{\mathbf{S}}^k(\tau)} \right\| d\tau \tag{12}$$

In (12) $\hat{\mathbf{S}}^k(\tau)$ is the homogenized effective stress vector under k_{th} strain-controlled case at parametric time τ and $\tilde{\mathbf{S}}^k(\boldsymbol{\alpha},\tau)$ is the second Piola-Kirchoff stress from the proposed material model with a realization of coefficients $\boldsymbol{\alpha} = (\lambda, \mu, \alpha, \beta, \gamma)$.

MATERIAL PARAMETERS FOR TRANSVERSELY ISOTROPIC YARN MODEL

The proposed homogenization techniques are first applied to an aligned-fiber yarn-composite using the 3D FE model of 8,288 10-noded tri-quadratic tetrahderal elements with 15,073 nodes (Figure 2). The yarn-composite is made up of aligned E-glass fibers in a hexagonal packing arrangement with a volume fraction of 76.6%. The epoxy matrix phase has a volume fraction of 23.4%. Four cases of finite deformation-controlled loading are applied to the unit cell model. The optimum agreement between homogenized stresses and those produced by the transversely isotropic hyperelasticity model are as shown in Figure 3. The associated material constants in the transversely-isotropic hyperelastic model of yarn-composite are shown in Table 1.

When individual components of the homogenized Green-Lagrange strain tensor are less than 10%, the transversely isotropic neo-Hookean model agrees quite well with the homogenized stress-strain responses computed from unit cell analysis of the fibers and matrix comprising the yarns. For cases of transverse compressive Green-Lagrange strain components E_{11}or E_{22} in excess of 10%, the homogenized stress response from unit cell analysis and that from the transversely isotropic material model start to deviate. This is due to a secondary geometrical effect of fiber-lockup wherein the interaction between fibers become significant as they approach a condition of mutual contact. Presently, we focus on range of strains where the homogenized macro-strains of the yarn composite are less than 10%.

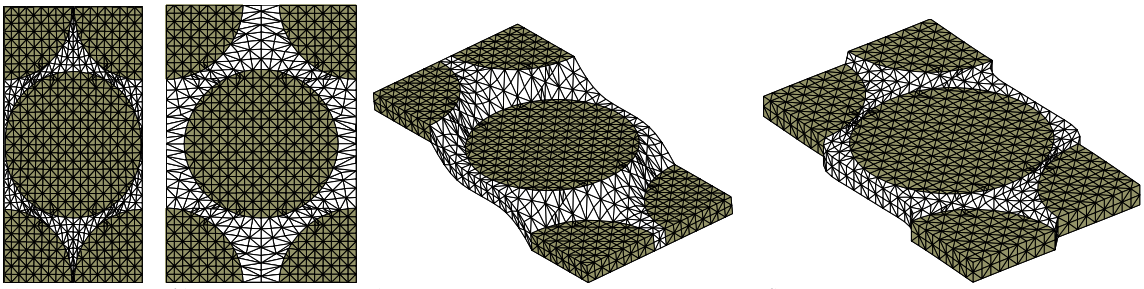

Figure 2. Deformed mesh of yarn-composite in hexahegonal arrangement: a) in-plane compression (F_{11}=0.9, other components zero); b) in-plane tension (F_{11}=1.1, others vanish); c) out-of-plane shear (F_{23}=F_{32}=0.1, others zero); and d) in-plane shear (F_{12}= F_{21}=0.1, others zero).

Table 1. Material parameters fiber and epoxy polymer matrix, and computed material parameters for the yarn composite.

E-glass fiber		Epoxy matrix		Yarn Composite Properties(GPa)				
E	ν	E	ν	μ	λ	α	β	γ
72.4 (GPa)	0.2	2.76 (GPa)	0.35	12.3	6.92	0.465	-0.498	4.69

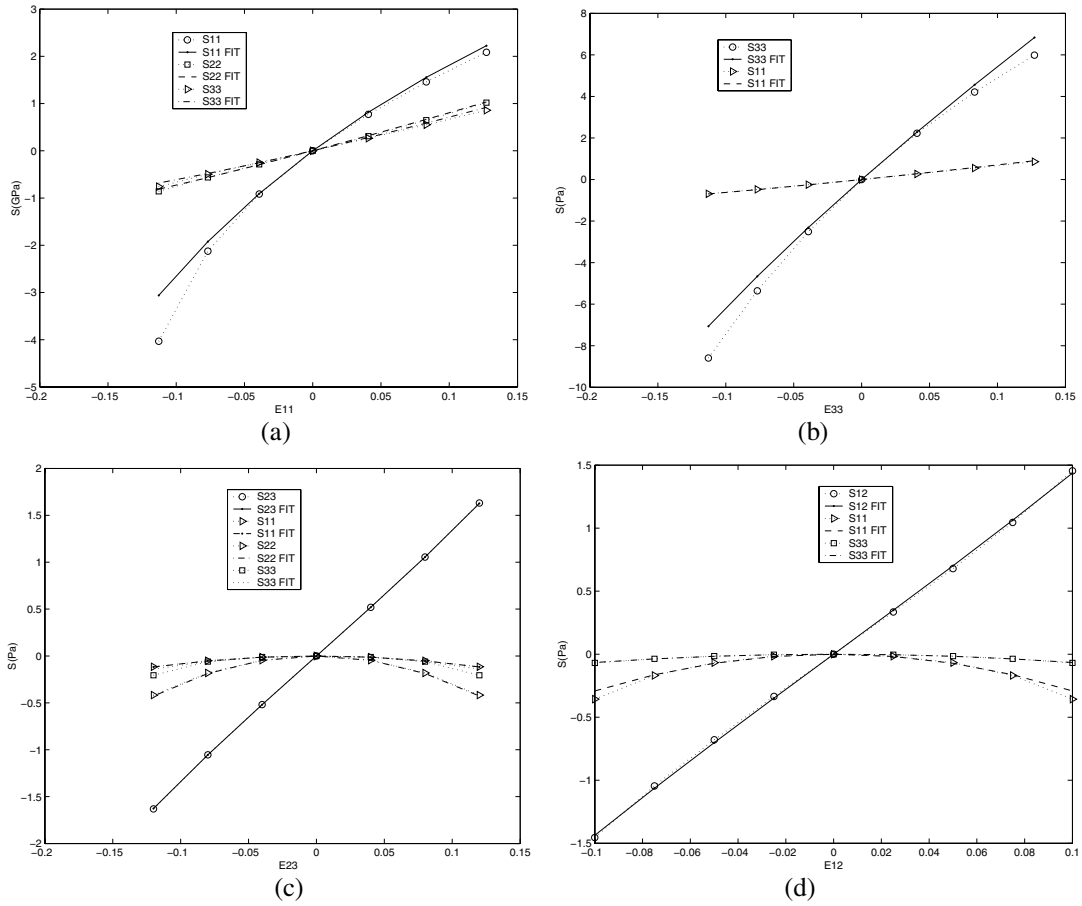

Figure 3. Strain-stress graph of textile composite implemented transversely- isotropic hyper-elasticity: a) in-plane constrained tension and compression (F_{11} controlled, others zero); b) out-of-plane tension and compression (F_{33} controlled, others zero); c) out-of-plane constrained shear (F_{23} =F_{32} controlled, others zero); and d) in-plane constrained shear (F_{12} =F_{21} controlled, others zero)

UNIT CELL ANALYSIS OF PLAIN-WEAVES AT FINITE DEFORMATIONS

Unit cell analysis is performed once again at the length scale of the plain-weave textile's wavelengths. Using the meshing techniques described by Kim (2002) a three-dimensional unit cell model for a plain-weave textile composite with a 36% yarn volume-fraction and 64% matrix volume-fraction is considered (Figure 4). The model employs 39,412 tri-quadratic tetrahedral elements and 58,221 nodes. The yarns are modeled as a homogenized transversely isotropic neo-Hookean solid, where the material directors vary smoothly along the length of yarns. With this model, each finite element comprising the yarn is given a unit director specifying the fiber-orientation that is sampled at the centroid of the element. Using deformation-controlled loading, the resulting unit cell analysis problems are solved with a diagonally pre-conditioned memoriless BFGS solver (Swan and Kosaka, 1997).

To study stiffness behaviors of plain-weave textile composites, two finite deformation loading cases, one of in-plane uniaxial compression, and one of in-plane uniaxial tension, are applied.

Periodicity of displacement field holds only in the in-plane directions while the top and bottom faces of the unit-cell are traction-free. Due to symmetry of the applied loading conditions and the symmetry of the unit-cell, only one quarter of full unit-cell was needed in these computations, the deformed meshes of which are shown in Figure 4, and the resulting stresses/strains of which are shown in Figure 5.

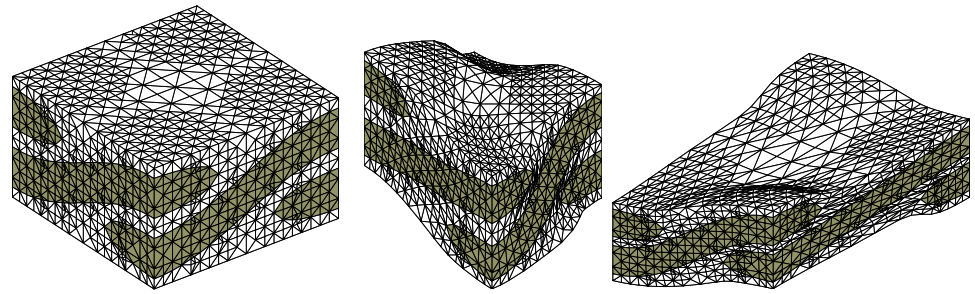

(a) (b) (c)

Figure 4. a) undeformed unit-cell model of plain-weave textile composite
b) deformed under compression; c) deformed under tension.

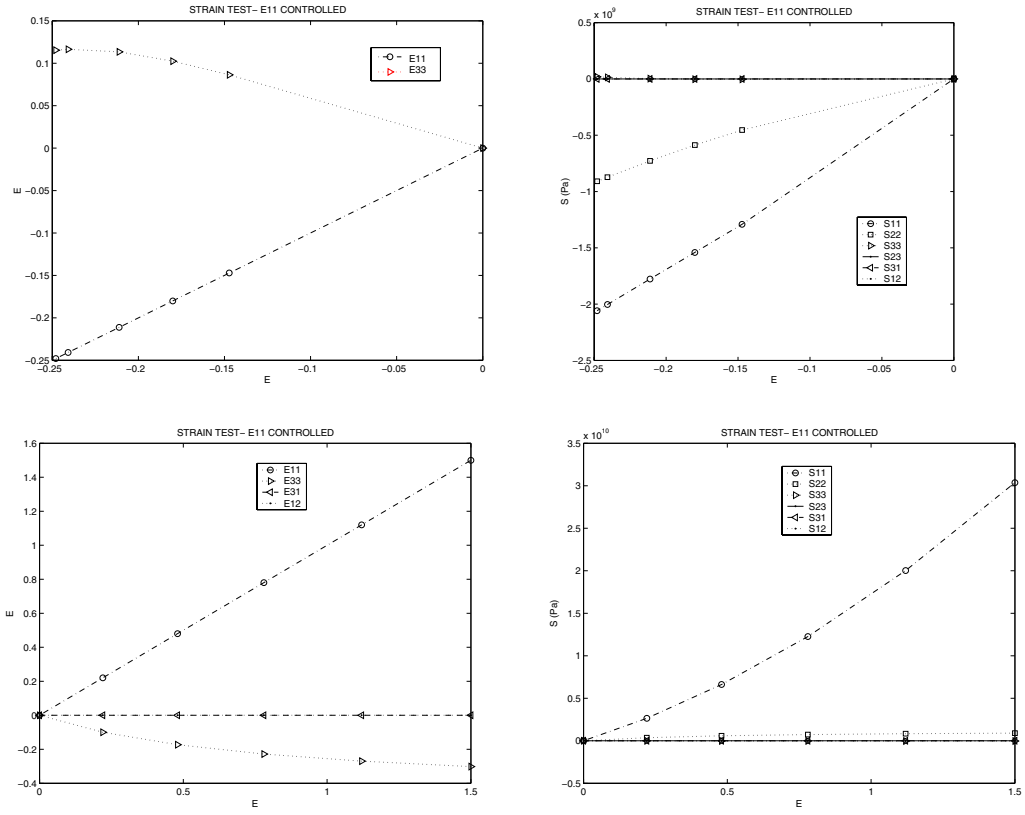

Figure 5. (a) resulting macroscopic strains in unit cell due to applied compression in X_1 direction; (b) stress-strain response in compression; (c) macroscopic strains under applied tension loading in X1 direction; (d) stress-strain response in tension.

The macroscopic stress-strain plots in Figure 5b indicate that material-scale geometric nonlinearity effects under in-plane compression become significant only at applied strains of approximately 25% at which point the yarns become unstable and are on the verge of buckling, whereas the corresponding stress-strain plots in 5d indicate that such effects become pronounced only at in-plane tensile strains in excess of 25%. In both cases, the textile composite would have failed at much smaller strains due to material failure and fracture in both the yarn and matrix phases. In subsequent extensions of this work both material failure and associated finite deformations at the material scale need to be addressed.

ACKNOWLEDGEMENTS

This work was funded by National Science Foundation CMS-9713335 and CMS-9896284. This support is gratefully acknowledged.

REFERENCES

Bonet, J. and Burton, A.J., (1998), "A simple orthotropic, transversely isotropic hyperelastic constitutive equation for large strain computations," Comput. Meth. Appl. Mech. Engrg. 162 (1-4), pp.151-164.

Fish, J. and Shek, K., (2000), "Multiscale analysis of composite materials and structures," Compos. Sci. Technol., Vol. 60 (12-13), pp. 2547-2556.

Jiang, Y., Tabiei, A. and Simites, J., (2000), "A novel micro-mechanics based approach to the derivation of constitutive equations for local/global analysis of plane weave fabric composites," Composites Science and Technology, Vol. 60, pp. 1825-1833.

Kim, H.J, (2002), Ph.D Dissertation, College of Engineering, University of Iowa, Iowa City, Iowa, USA.

Nemat-Nasser S., (1999), "Averaging theorems in finite deformation plasticity," Mechanics of Materials, Vol. 31(8) pp. 493-523.

Peng, X. and Cao, J., (2002), "A dual homogenization and finite element approach for material characterization of textile composites," Composites: Part B Vol. 33, 45—56.

Swan C.C., (1994), "Techniques for stress and strain controlled homogenization of inelastic periodic composites," Comput. Methods Appl. Mech. Engrg. 117: 249-267.

Swan C.C. and Kosaka I., (1997), "Homogenization-based analysis and design of composites," Computers and Structures, Vol. 64, pp.603-621.

Tabiei, A. and Jiang, Y., (1999), "Woven fabric composite material model with material nonlinearity for nonlinear finite element simulation", Int. J. Solids. Struct. Vol. 36 (18), pp. 2757-2771.

Takano, N., Ohnishi, Y., and Zako, M., (2001), "Microstructure-based deep-drawing simulation of knitted fabric reinforced thermo plastics by homogenization theory," Int. J. Solids Struct. Vol.38 (36-37), pp. 6333-6356.

Weiss, J.A. Maker, B.N. and Govindjee, S., (1996), "Finite element implementation of incompressible transversely isotropic hyperelasticity, Comput. Meth. Appl. Mech. Engrg., Vol. 135(1-2), pp. 107-128.